

High Glucose Suppresses Osteogenic Differentiation and Induces Mitochondrial Dysfunction in Osteoblasts via SIRT1/RECQL4 Axis; A Laboratory Study Using Mouse Cells

Xiahui Zhou¹, Weixiong Peng², Shenglian Pan³, Zhe Lin², Rongrong Pan⁴, Qinglai Wang^{2,*}

¹National Office for Drug Clinical Trials, Wenzhou Hospital of Traditional Chinese Medicine Affiliated to Zhejiang Chinese Medicine University, 325000 Wenzhou, Zhejiang, China

²Orthopedics and Traumatology Department of TCM, Wenzhou Hospital of Traditional Chinese Medicine Affiliated to Zhejiang Chinese Medicine University, 325000 Wenzhou, Zhejiang, China

³Department of Acupuncture and Massage, Wenzhou Hospital of Traditional Chinese Medicine Affiliated to Zhejiang Chinese Medicine University, 325000 Wenzhou, Zhejiang, China

⁴Department of Geriatrics, Wenzhou Hospital of Traditional Chinese Medicine Affiliated to Zhejiang Chinese Medicine University, 325000 Wenzhou, Zhejiang, China

*Correspondence: wangqinglai_wql@163.com (Qinglai Wang)

Published: 20 August 2022

Background: Diabetes mellitus has an adverse effect on human bones, which is a risk factor for osteoporosis. The aim of this study was to explore the mechanism of the effects of high glucose (HG) on the osteogenic differentiation of osteoblasts.

Methods: In this study, mouse MC3T3-E1 cells were cultured in high glucose level at 30 mM with 24.5 mM mannitol and 5.5 mM glucose as control. Plasmid circular deoxyribonucleic acids (pcDNAs) and small interference ribonucleic acids (RNAs) were transfected for functional analysis of RecQ helicase-like 4 (RECQL4) and sirtuin 1 (SIRT1). The viability, alkaline phosphatase (ALP) activity, and OCN (provide in full) concentration was measured via methyl thiazolyl tetrazolium (MTT), colorimetric, enzyme-linked immunosorbent assay (ELISA) assays. Mitochondrial functions were assessed by mitochondrial membrane potential (MMP) and the levels of adenosine triphosphate (ATP), glutathione (GSH), and malondialdehyde (MDA). Quantitative reverse-transcription polymerase chain reaction or western blot were conducted to detect the gene or protein expression. RECQL4 acetylation assay was performed and the interaction between RECQL4 and SIRT1 was detected via co-immunoprecipitation assay.

Results: The effects of HG on downregulating cell viability, the levels of osteogenic differentiation-related markers (ALP and OCN), p53 phosphorylation, ATP and GSH as well as RECQL4 and apoptosis-related factors (Cytochrome C and Cleaved caspase-3) upregulating MMP loss and MDA content were reversed following RECQL4 over expression ($p < 0.01$). Sirtuin 1 (SIRT1) over expression promoted the viability and the levels of ALP and OCN, while silencing RECQL4 did the opposite ($p < 0.05$) and caused a reversion in HG-treated osteoblasts ($p < 0.01$). Additionally, silencing SIRT1 inhibited the acetylation of RECQL4 ($p < 0.01$) and the interaction between SIRT1 and RECQL4.

Conclusions: HG repressed the osteogenic differentiation and downregulated MMP via SIRT1/RECQL4 axis in osteoblasts.

Keywords: diabetes mellitus; high glucose; osteogenic differentiation; sirtuin 1; RecQ helicase-like 4; deacetylation

Introduction

Diabetes mellitus (DM) is a metabolic disease characterized by chronic hyperglycemia, as a result of insulin defection or deficiency. The disease is not only one of the most prevalent chronic medical conditions but also recognized as a cardiovascular major risk factor, which is related to increase on both cardiovascular morbidity and mortality [1,2]. Accumulating evidence pointed out that the disease has an adverse effect on human bones as well, which is associated with an increase on the risk of osteoporosis [3]. These comorbidities pose economical burden and cause a

negative impact on the life quality of patients, which necessitate ameliorative strategy [4].

Some clinical disorders of availability on substrate, DM for instance, are responsible for the dysfunction on osteoblasts. Osteoblasts are cells located in the inner layer of the periosteum and play a prodigal role in bone repair and growth. Dysfunction of these cells results in the fragility of skeleton and the onset of fracture [5,6]. It has been suggested that HG inhibits the proliferation and osteogenic differentiation of osteoblasts and is related to fracture and increase on the apoptosis of osteoblasts [7–9].

The aim of this study was therefore to investigate the mechanism implicated. RecQ helicase-like 4 (RECQL4), a member of RECQ family [10], is required for normal osteoblast expansion and osteosarcoma formation [11]. Additionally, RECQL4 can play a pivotal role in skeletal development in mice [12]. Lack of the mitochondrial functions of RECQL4 leads to aerobic glycolysis [13]. Aerobic glycolysis is an energy-inefficient process, that requires large amounts of glucose. Therefore, it is speculated that the effect of RECQL4 on mitochondrial function is involved in DM-related orthopedic diseases.

Reversible acetylation on the protein in the mitochondria has been underlined as a major modulatory mechanism to control the function of protein, and it has been revealed that the acetylation of the non-histone protein participates in several cellular processes associated with the physiology and disease, like DNA (deoxyribonucleic acid) damage repair and metabolism, for instance [14,15].

Meanwhile, it shouldn't be neglected that under the condition of HG, the succeeding oxidative stress results in the repression on the level of sirtuin deacetylase and the increase on histone acetylation [16]. Additionally, it has been suggested that oxidative stress and possible oxidative DNA damage cause the acetylation of RECQL4 and that sirtuin 1 (SIRT1), an NAD⁽⁺⁾-dependent deacetylase promoting the osteogenic differentiation in mice, could interact with and deacetylate RECQL4 [17–19]. Accordingly, it was hypothesized that the SIRT1-mediated deacetylation of RECQL4 was implicated in the mechanism via which HG caused a disruption in osteoblasts.

Materials and Methods

Cell Culture and Processing

Mouse osteoblast cell line MC3T3-E1 (iCell-m031, iCell, Shanghai, China) was cultured in α -minimum essential medium (α -MEM, 12561-056, Gibco, Waltham, MA, USA) supplemented with 10% fetal bovine serum (FBS, 16140-063, Gibco, Waltham, MA, USA) and 1% penicillin-streptomycin (15070-063, Gibco) at 37 °C, 5% CO₂. Then, MC3T3-E1 cells were divided into the following groups: Control group, Man group and HG group. Mannitol was used as osmotic pressure control. MC3T3-E1 cells in control group were treated with 5.5 mM D-Glucose (G116303, Aladdin, Shanghai, China), and cells in mannitol (Man) group were treated with 24.5 mM mannitol (M108829, Aladdin, Shanghai, China) and 5.5 mM D-glucose. In addition, cells in HG group were respectively treated with 15, 30, and 50 mM D-Glucose.

Transfection

RECQL4 and SIRT1 were successfully over expressed using pcDNA3.1 plasmid (VT1001, YouBio, Changsha, China) and empty pcDNA3.1 plasmid was used for negative control (NC), while the small interfering RNA (siRNA)

against RECQL4 (siRECQL4, siG170516084950-1-5, target sequence: 5'-CGCAGTCTATGCCAAAACAGAGC-3') and the negative control (siNC, siN0000002-1-5, target sequence: 5'-CGCCAACAGTAAAGCGCAGCTAT-3') were constructed and ordered from RiboBio (Guangzhou, China).

1×10^6 cells/well MC3T3-E1 cells were cultured in a 6-well plate until became 80% confluent, and the transfection was carried out via Lipofectamine 3000 transfection reagent (L3000-001, Invitrogen, Carlsbad, CA, USA) at 37 °C in line with the protocols provided by the manufacturer. Two days (48 h) later, cells were harvested for later studies.

MTT Assay

MC3T3-E1 cells were grown in (ninety-six well plates) 96-well plates at a density of 2×10^3 cells/well at 37 °C with 5% CO₂, and then treated with/without D-glucose or mannitol for 24, 48 and 72 h. 10 μ L MTT reagent (C0009S, Beyotime, Shanghai, China) with non-serum medium were added at 37 °C for 4 h, and the formazan crystal formed was dissolved via the solvent provided with the kit. The OD value was recorded via a microplate photometer (51119180ET, Thermo Fisher Scientific, Waltham, MA, USA) at an absorbance of 570 nm.

Alkaline Phosphatase (ALP) Activity

ALP activity in the osteoblasts was measured in line with previous study [20]. At a density of 2×10^5 cells/well, MC3T3-E1 cells were cultured in 6-well plates within osteogenic inductive medium (α -MEM with 10% FBS, 10^{-8} M dexamethasone (D137736, Aladdin, Shanghai, China), 50 mg/L ascorbic acid (A103539, Aladdin, Shanghai, China) and 10 mM β -glycerophosphate (G9422, Sigma-Aldrich, St Louis, MO, USA) after required processing. After incubation for 7 days, cells were scraped into 1% Triton X-100 (T109026, Aladdin, Shanghai, China), sonicated and centrifugated at 12,000 \times g for 10 min. ALP activity was determined by an ALP assay kit (ab83369, Abcam, Cambridge, UK) according to the protocols provided by the manufacturer, and the absorbance was recorded at 520 nm using a microplate photometer.

Enzyme-Linked Immunosorbent Assay (ELISA)

At a density of 1×10^5 cells/well, MC3T3-E1 cells were cultured in 96-well plates, at 37 °C with 5% CO₂ for 24 h. Then, after the collection of cell culture media, the level of osteocalcin (OCN) was quantified using the corresponding ELISA kit (60-1305, Quidel, San Diego, CA, USA). Specifically, the sample cell culture media was diluted as advised, following which 50 μ L biotinylated antibody against OCN was pipetted and incubated with the sample on a horizontal rotator at room temperature for 1 h. The contents of each well were then aspirated and horseradish peroxidase (HRP)-conjugated antibody against OCN was introduced for an incubation on a horizontal rotator at room

temperature for 1 h in the dark. The aspiration of the contents was repeated and ELISA HRP substrate was added for further incubation on a horizontal rotator at room temperature for 30 min, followed by the addition of 50 μ L ELISA stop solution for a 1-min mixture. OD value at an absorbance of 450 nm was measured by a microplate photometer.

Assessment on Mitochondrial Membrane Potential (MMP)

MMP was assessed using JC-1 mitochondrial membrane potential assay kit (C2006, Beyotime, Shanghai, China) following a prior study [21]. MC3T3-E1 cells were collected after required treatment, then 5 μ M JC-1 staining kit were added to the cells for an incubation at 37 °C for 30 min in the dark. Finally, cells were analyzed using a flow cytometer (BR168323, Guava easyCyte Benchtop, Luminox, Austin, TX, USA) and Kaluza C (version 2.1, Beckman Coulter, Indianapolis, IN, USA).

Determination on the Levels of Adenosine Triphosphate (ATP), Glutathione (GSH) and Malondialdehyde (MDA)

ATP level was determined, as previously described [22]. ATP levels were measured with ATP fluorometric assay kit (K354, BioVision, Milpitas, CA, USA) according to the protocols of the producer. In brief, MC3T3-E1 cells were harvested after treatment and transfection and were subjected to homogenization in 100 μ L ATP assay buffer provided in the kit. After that, 50 μ L of deproteinized cell lysate was mixed with 50 μ L reaction mix in 96-well plates containing ATP probe, converter and developer. The mixture was then incubated at room temperature for 30 min, and optical density (OD) value at 570 nm was determined using a microplate photometer.

GSH level was measured, in line with the technique described in a previous publication [23]. After different treatment, 1×10^6 MC3T3-E1 cells were harvested, and GSH level was measured by a glutathione reductase/5, 5'-dithiobis-(2-nitrobenzoic acid) (DTNB) reagent (D105559, Aladdin, Guangzhou, China). In brief, GSH level was determined within a reaction mixture which contained 50 μ L cell lysates, 50 μ L DTNB and μ L GSH reductase (G105427, Aladdin, Guangzhou, China) in the assay buffer. After the incubation at 25 °C for 5 min, the reaction was started via adding 50 μ L nicotinamide adenine dinucleotide phosphate (NADPH, 0.16 mg/mL, N276326, Aladdin, Guangzhou, China), and OD value at 412 nm was recorded with a microplate photometer.

MDA level was quantified by the concentration of thiobarbituric acid-reactive substance (TBRS) assay, according to the technique described in a previous study [24]. In detail, the supernatant of MC3T3-E1 cells after different treatment was collected, and then 0.2 mL of the supernatants was added into a 10 mL centrifuge tube

containing 1.5 mL 20% acetic acid (A116173, Aladdin, Guangzhou, China), 0.2 mL 8.1% sodium dodecyl sulfate (SDS, S108350, Aladdin, Guangzhou, China) and 1 mL 6% thiobarbituric acid (T108505, Aladdin, Guangzhou, China). The mixture was then heated within a boiling water for 45 min. 4 mL n-butanol (B111578, Aladdin, Guangzhou, China) was added into the mixture after cooling down, and the absorbance at 535 nm was recorded using a microplate photometer.

RECQL4 Acetylation Assay

MC3T3-E1 cells were co-transfected with the constructs for RECQL4 and SIRT1 for 36 h and lysed in the buffer containing NP-40 (0.5%, N274337, Aladdin, Guangzhou, China), glycerol (10%, G116210, Aladdin, Guangzhou, China), protease inhibitor cocktail (1 \times , P301903, Aladdin, Guangzhou, China), HEPES-KOH (50 mM, H301907, Aladdin, Shanghai, China), sodium chloride (500 mM, NaCl, S298765, Aladdin, Guangzhou, China), trichostatin A (TSA, 5 μ M, T129665, Aladdin, Guangzhou, China), nicotinamide (10 mM, N105043, Aladdin, Guangzhou, China) and sodium butyrate (10 mM, S102956, Aladdin, Guangzhou, China), followed by being sonicated on ice. Then, magnetic beads were used to pull down RECQL4 at 4 °C and sequentially washed in washing buffer A (NP-40 (0.5%), glycerol (10%), HEPES-KOH (50 mM), NaCl (500 mM), and nicotinamide (10 mM)), washing buffer B (NP-40 (0.5%), glycerol (10%), HEPES-KOH (50 mM), and NaCl (500 mM)) and washing buffer C (NP-40 (0.5%), glycerol (10%), HEPES-KOH (50 mM), NaCl (150 mM)). After that, the RECQL4 protein was eluted via the incubation of the beads in washing buffer C and analyzed with SDS-PAGE. Finally, the acetylation of RECQL4 was determined, using western blot with an antibody against acetylated lysine (#9441, CST, Danvers, MA, USA) [19].

Co-Immunoprecipitation (Co-IP) Assay

Specifically, MC3T3-E1 cells were co-transfected with siSIRT1 or/and vectors expressing FLAG-RECQL4. Cells were harvested 48 h after the transfection and lysed in IP lysis buffer (0.2% NP-40 (0.2%), magnesium chloride (MgCl₂, 2 mM, M283899, Aladdin, Guangzhou, China), NaCl (150 mM), Tris-Hydrochloride (HCl) buffer (40 mM, T197246, Aladdin, Guangzhou, China), and Triton X-100 (0.4%) with protease inhibitor and benzonase (E1014, 20 U/mL, Sigma-Aldrich, St Louis, MO, USA). Then, the lysates were incubated with protein G agarose beads (#37478, CST, Danvers, MA, USA) or FLAG-magnetic beads (M8823, Sigma-Aldrich, St Louis, MO, USA) at 4 °C overnight. After this, the beads were rinsed in washing buffer including NaCl (150 mM), Tris-HCl buffer (20 mM) and Triton X-100 (0.2%) six times, resuspended in SDS sample buffer and boiled at 95 °C. Subsequently, western blot was used to analyze the results after the beads were

eluted with the washing buffer mentioned above containing 3× FLAG® peptide (F4799, Sigma-Aldrich, St Louis, MO, USA), where the antibodies against RECQL4 (ab192375, 1:2000, Abcam, Cambridge, UK) and SIRT1 (#8469, CST, Danvers, MA, USA) were used, according to the technique described in a previous study [19].

Quantitative Reverse-Transcription Polymerase Chain Reaction (qRT-PCR)

Total RNA was extracted from cells, with the help of Trizol (R0016, Beyotime, Shanghai, China), and preserved in -80 °C. The concentration of extracted RNA was determined with a spectrophotometer (NanoDrop Lite, ND-LITE-PR, Thermo Fisher Scientific, Waltham, MA, USA). The polymerase chain reaction (PCR) was conducted using BeyoFast Probe One-Step qRT-PCR kit (D7277S, Beyotime, Shanghai, China) in a reverse-transcription PCR system (LMPCS-801, Labmate, Suffolk, UK) with the listed conditions: 50 °C for 30 min, 95 °C for 2 min, and 40 repeated cycles of 95 °C for 15 s and 60 °C for 30 s. The sequences of primers used were listed in Table 1. β -actin was used for the housekeeping gene. Relative expressions were later quantified via $2^{-\Delta\Delta C_t}$ calculation method [25].

Table 1. Primers for qRT-PCR.

Gene	Primers
SIRT1	
Forward	5'-GACTCCTCACTAATGGCTTT-3'
Reverse	5'-CACTTCATGGGGTATAGAAC-3'
ALP	
Forward	5'-CCTGGATCTCATCAGTATTT-3'
Reverse	5'-GTTGTTGTGAGCGTAATCTA-3'
OCN	
Forward	5'-GCAATAAGGTAGTGAACAGA-3'
Reverse	5'-ATACTGGTCTGATAGCTCGT-3'
Cytochrome C	
Forward	5'-AAAAAGTACATCCCTGGAAC-3'
Reverse	5'-TATTAGGTCTGCCCTTCTC-3'
β -actin	
Forward	5'-CTATGTTGCTCTAGACTTCG-3'
Reverse	5'-ATAGAGGTCTTACGGATGTC-3'

Western Blot

Protein expressions were determined as previously described [19]. After cell collection, the of lysis and extraction of total protein were conducted using RIPA lysis buffer (P0013C, Beyotime, Shanghai, China), and the concentration of extracted protein was measured by BCA protein assay kit (P0012S, Beyotime, Shanghai, China). Following the completion of electrophoresis and transfer onto polyvinylidene fluoride (PVDF) membrane (FFP36, Beyotime, Shanghai, China), the membrane containing protein was blocked by fat-free milk (5%) for 2 h and incu-

bated with the primary antibodies, including those against RECQL4, p53 (ab26, 1:2000, Abcam, Cambridge, UK), phosphorylated (p)-p53 (#82530, 1:1000, CST, Danvers, MA, USA), Cytochrome C (ab90529, 1:200, Abcam, Cambridge, UK), Cleaved caspase-3 (ab2302, 1:1000, Abcam, Cambridge, UK), Caspase-3 antibody (ab2302, 1:1000, Abcam, Cambridge, UK), and housekeeping control β -actin (ab8226, 1:2000, Abcam, Cambridge, UK) at 4 °C overnight. After that, the membrane was incubated in secondary HRP-conjugated antibodies: goat anti-rabbit IgG H&L (1:2000, #7074, CST, Danvers, MA, USA) and goat anti-mouse IgG H&L (1:2000, A0216, Beyotime, Shanghai, China) at room temperature for 1 h and rinsed in TBST (T196393, Aladdin, Shanghai, China) thrice. The visualization of protein band was performed using an enhanced chemiluminescence (ECL) kit (P0018FS, Beyotime, Shanghai, China) and an imaging system (GelView 6000Plus, Biolight Biotechnology, Guangzhou, China). Data on grey values were calculated using ImageJ (version 5.0, Bio-Rad, Hercules, CA, USA).

Statistical Analysis

Each experiment was performed in independent triplicate. Normally distributed continuous data were described as mean \pm standard deviation and analyzed using Graphpad software (version 8.0, Graphpad, Inc., La Jolla, CA, USA). Kolmogorov-Smirnov test was used to verify normality. Comparison of more than two groups of normally distributed continuous data was carried out using one-way analysis of the variance ANOVA followed by Bonferroni *post hoc* test. When a statistically significant difference was detected between more than two groups, each pair was compared. Statistical significance was set as *p*-value was below 0.05.

Results

HG Suppressed the Viability and Downregulated RECQL4 Expression in Osteoblasts

This information belongs to the method According to the results, HG treatment led to a decreased OD value (Fig. 1A, *p* < 0.05). It was suggested that the viability of MC3T3-E1 cells was suppressed evidently when cells were treated with 30 mM D-glucose [7], and 30 mM D-glucose was thus used for subsequent studies. A same inhibitory effect on cell viability was found after MC3T3-E1 cells were treated with 30 mM D-glucose (Fig. 1B, *p* < 0.01). The osmotic pressure, which was created by mannitol and was equivalent to HG conditions, had no effect on the OD value (Fig. 1B). These results suggested that HG suppressed the viability of osteoblasts. In addition, in comparison with the Man group, in the control group, no statistically significant difference in cell viability was observed (Fig. 1B).

Then, this information belongs to the method It was found that the expression of RECQL4 was significantly

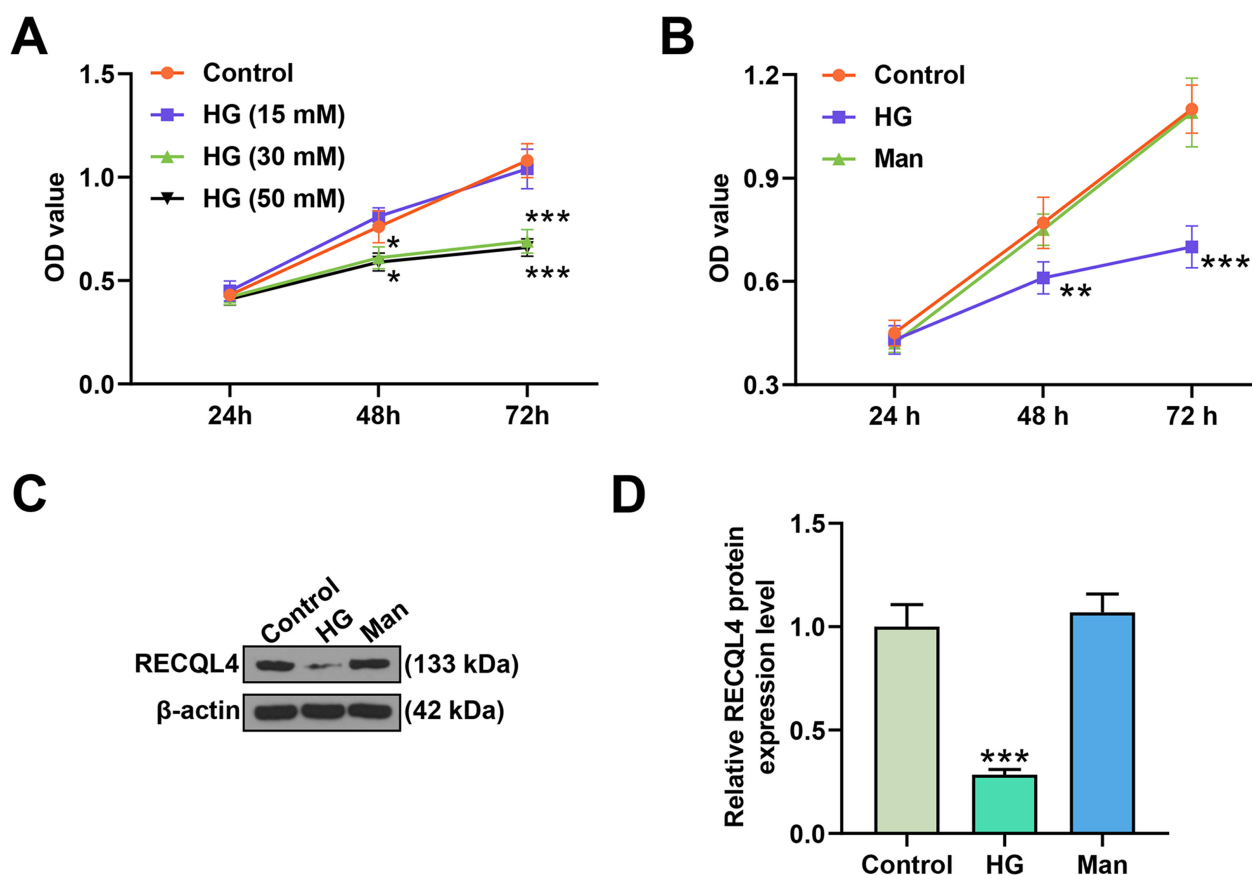


Fig. 1. HG suppressed the viability and repressed RECQL4 expression in osteoblasts. * $p < 0.05$, ** $p < 0.01$, *** $p < 0.001$, vs. control.

downregulated after the treatment of HG (Fig. 1C,D, $p < 0.001$).

RECQL4 Reversed the Effects of HG on Cell Viability, Osteogenic Differentiation Markers Level and p53 Expression in Osteoblasts

This information belongs to the method. It was found that HG treatment resulted in a significantly decreased OD value in MC3T3-E1 cell, whereas RECQL4 overexpression caused a significant increase in OD value and reversed the effects of HG (Fig. 2A, $p < 0.05$).

This information belongs to the method. In MC3T3-E1 cells, after HG treatment, both ALP activity and OCN content were significantly downregulated, and ALP and OCN expressions were significantly decreased as well (Fig. 2B–D, $p < 0.001$). However, RECQL4 overexpression significantly upregulated ALP activity and OCN content as well as ALP and OCN expressions in MC3T3-E1 cells, in addition to the suggestion that RECQL4 overexpression reversed the effects of HG on ALP and OCN levels in MC3T3-E1 cells (Fig. 2B–D, $p < 0.05$).

This information belongs to the method. It was demonstrated that the expression of p-p53 after HG treat-

ment was significantly increased, and p-p53/p53 ratio was significantly raised as well, whereas RECQL4 overexpression significantly decreased both p-p53 expression and p-p53/p53 ratio and reversed the effects of HG in MC3T3-E1 cells (Fig. 2E–G, $p < 0.001$).

RECQL4 Reversed the Effects of HG on MMP Loss and the Levels of ATP, GSH and MDA in Osteoblasts

This information belongs to the method. After HG treatment, MMP loss and the content of MDA were significantly up-regulated, whereas the level of ATP and the content of GSH were significantly down-regulated (Fig. 3A–E, $p < 0.001$). However, RECQL4 overexpression led to significantly reduced MMP loss and MDA content yet significantly increased ATP level and GSH content (Fig. 3A–E, $p < 0.05$). Furthermore, RECQL4 significantly diminished the effects of HG on MMP loss and the levels of ATP, GSH and MDA in osteoblasts (Fig. 3A–E, $p < 0.05$).

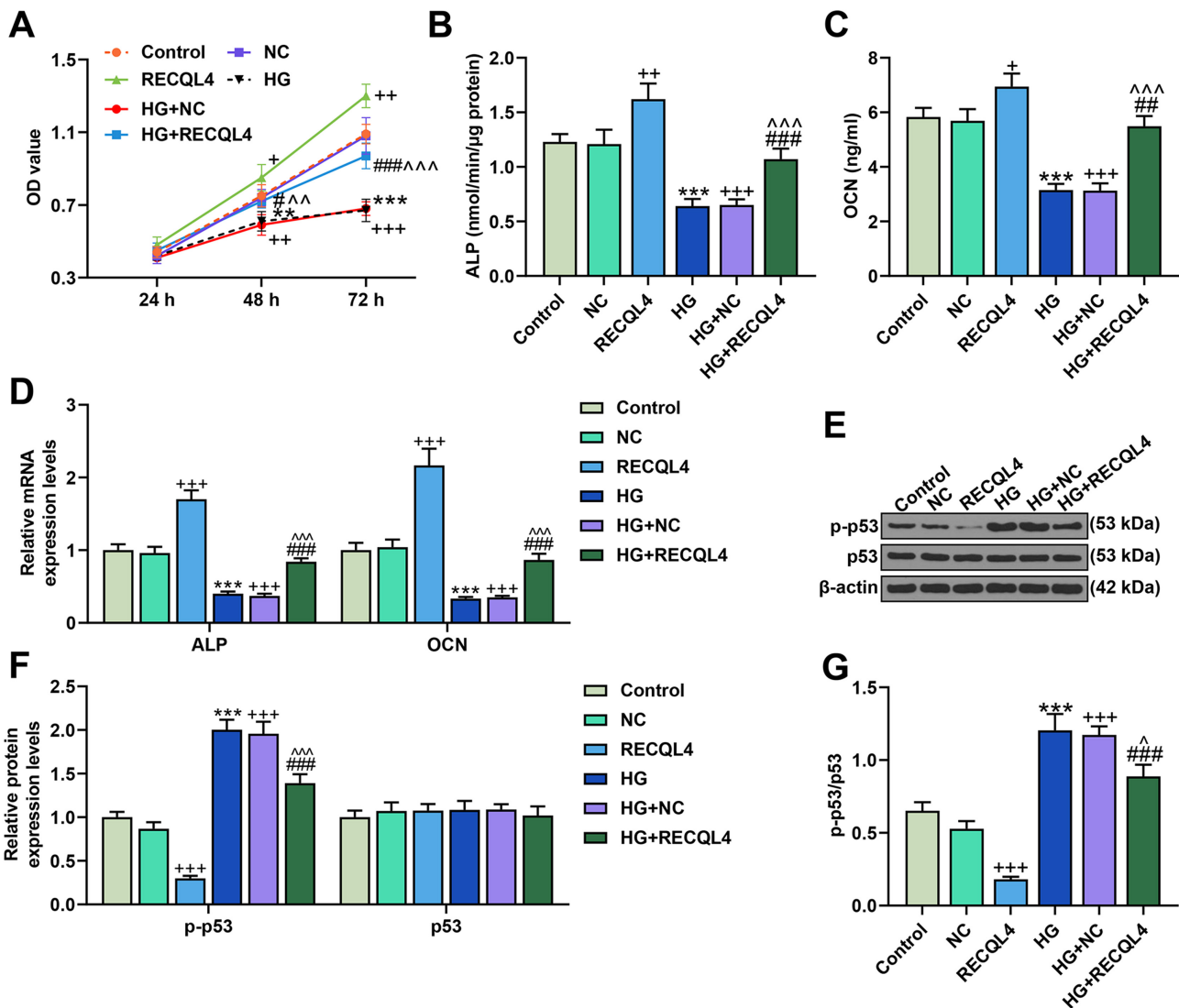


Fig. 2. RECQL4 reversed the effects of HG on the viability and the levels of osteogenic differentiation markers and p53 in osteoblasts. $^+p < 0.05$, $^{++}p < 0.01$, $^{+++}p < 0.001$, vs. NC; $^{**}p < 0.01$, $^{***}p < 0.001$, vs. Control; $^{\#}p < 0.05$, $^{\#\#}p < 0.01$, $^{\#\#\#}p < 0.001$, vs. RECQL4; $^{\wedge}p < 0.05$, $^{\wedge\wedge}p < 0.01$, $^{\wedge\wedge\wedge}p < 0.001$, vs. HG+NC.

RECQL4 Reversed the Effects of HG on the Expressions of RECQL4 and Apoptosis-Related Factors in Osteoblasts

This information belongs to the method. After HG treatment, the level of RECQL4 was significantly decreased yet those of cytochrome C and cleaved caspase-3 were significantly increased. On the other hand, RECQL4 over expression did the opposite (Fig. 4A–D, $p < 0.05$). A statistically significant increase in cleaved caspase-3/caspase-3 ratio was observable after HG treatment, whereas a statistically significant decrease was shown following the over expression of RECQL4 (Fig. 4B–D, $p < 0.001$). In addition, RECQL4 abolished the effects of HG on the expressions of RECQL4 and apoptosis-related factors in osteoblasts (Fig. 4A–D, $p < 0.05$).

Silencing RECQL4 Neutralized the Effects of SIRT1 on the Level of Osteogenic Differentiation-Related Factors in HG-treated Osteoblasts

This information belongs to the method. A significantly lower-expression of SIRT1 was found in HG-treated MC3T3-E1 cells (Fig. 5A–C, $p < 0.001$). Also, the over expressed SIRT1 significantly increased the OD value and significantly enhanced the levels of ALP and OCN in HG-treated MC3T3-E1 cells. On the other hand, whilst the silence explain what does this mean of RECQL4 did the exact opposite and counteracted the effects of SIRT1 in HG-treated MC3T3-E1 cells (Fig. 5D–H, $p < 0.05$).

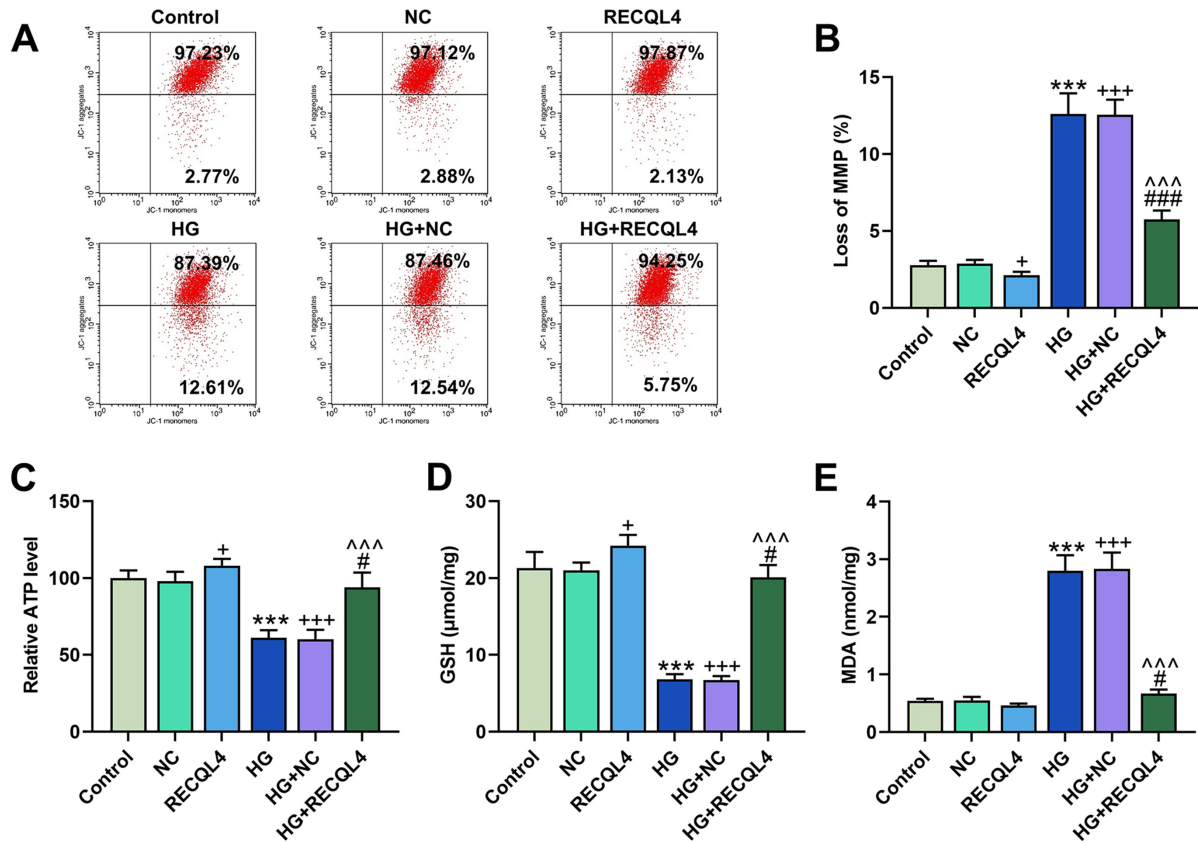


Fig. 3. RECQL4 reversed the effects of HG on mitochondrial function in osteoblasts. $^+p < 0.05$, $^{+++}p < 0.001$, vs. NC; $^{***}p < 0.001$, vs. control; $^{\#}p < 0.05$, $^{###}p < 0.001$, vs. RECQL4; $^{\wedge\wedge}p < 0.001$, vs. HG+NC.

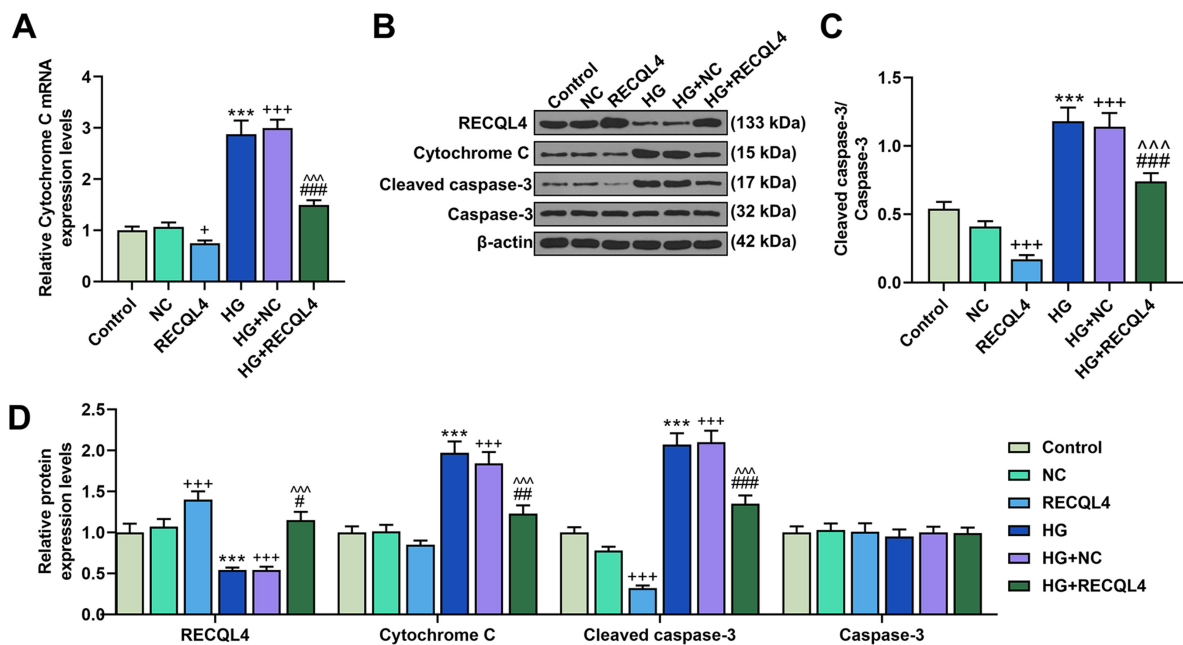


Fig. 4. RECQL4 reversed the effects of HG on the expressions of RECQL4 and apoptosis-related factors in osteoblasts. $^+p < 0.05$, $^{++}p < 0.01$, $^{+++}p < 0.001$, vs. NC; $^{***}p < 0.001$, vs. control; $^{\#}p < 0.05$, $^{##}p < 0.01$, $^{###}p < 0.001$, vs. RECQL4; $^{\wedge}p < 0.01$, $^{\wedge\wedge}p < 0.001$, vs. HG+NC.

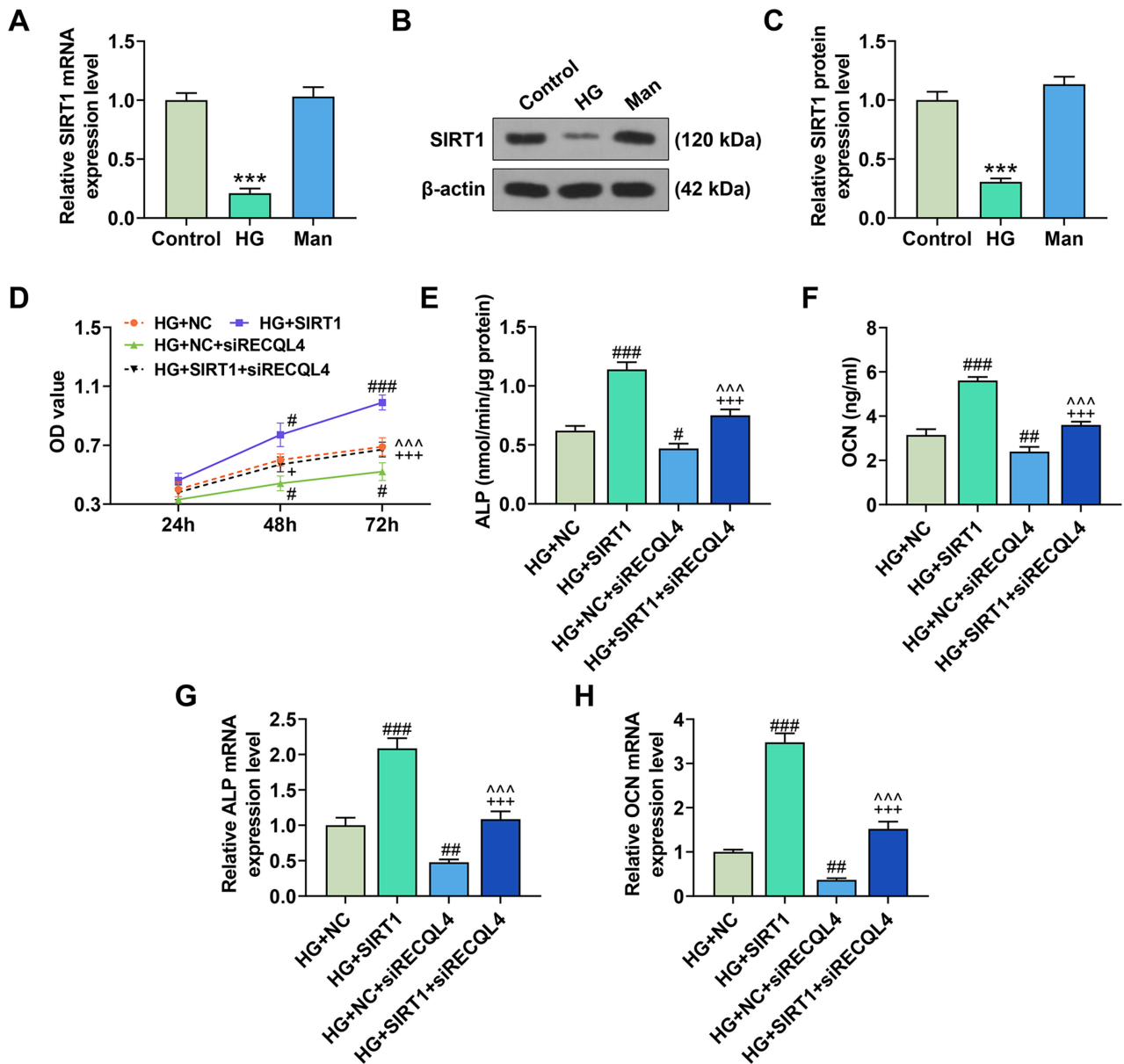


Fig. 5. Silencing RECQL4 neutralized the effects of SIRT1 on the level of osteogenic differentiation-related factors in HG-treated osteoblasts. *** $p < 0.001$, vs. control; # $p < 0.05$, ### $p < 0.01$, #### $p < 0.001$, vs. HG+NC; + $p < 0.05$, +++ $p < 0.001$, vs. HG+SIRT1; ^^ $p < 0.001$, vs. HG+NC+siRECQL4.

SIRT1 Interacted with and Deacetylated RECQL4 in HG-treated Osteoblasts

This information belongs to the method. Following the silence of SIRT1, the level of acetylated RECQL4 significantly increased, those treated with HG in particular (Fig. 6A,B, $p < 0.01$). On the other hand, the over expressed SIRT1 significantly repressed the level of acetylated RECQL4, and the silence of RECQL4 did the same (Fig. 6C,D, $p < 0.01$). Besides, the over expression of SIRT1 and silence of RECQL4 significantly decreased the level of acetylated RECQL4 in HG-treated osteoblasts (Fig. 6C,D, $p < 0.05$). In addition, the results of Co-IP assay

suggested that the interaction between acetylated RECQL4 and SIRT1 was significantly promoted in HG-treated osteoblasts following the silence of SIRT1 (Fig. 6E,F).

Discussion

The aim of this study was to explore the mechanism of the effects of HG on the osteogenic differentiation of osteoblasts. The study showed HG repressed the osteogenic differentiation and induced mitochondrial dysfunction via SIRT1/RECQL4 axis in osteoblasts. In this study, HG significantly suppressed the levels of osteogenic differentiation-related markers ALP and OCN yet enhanced

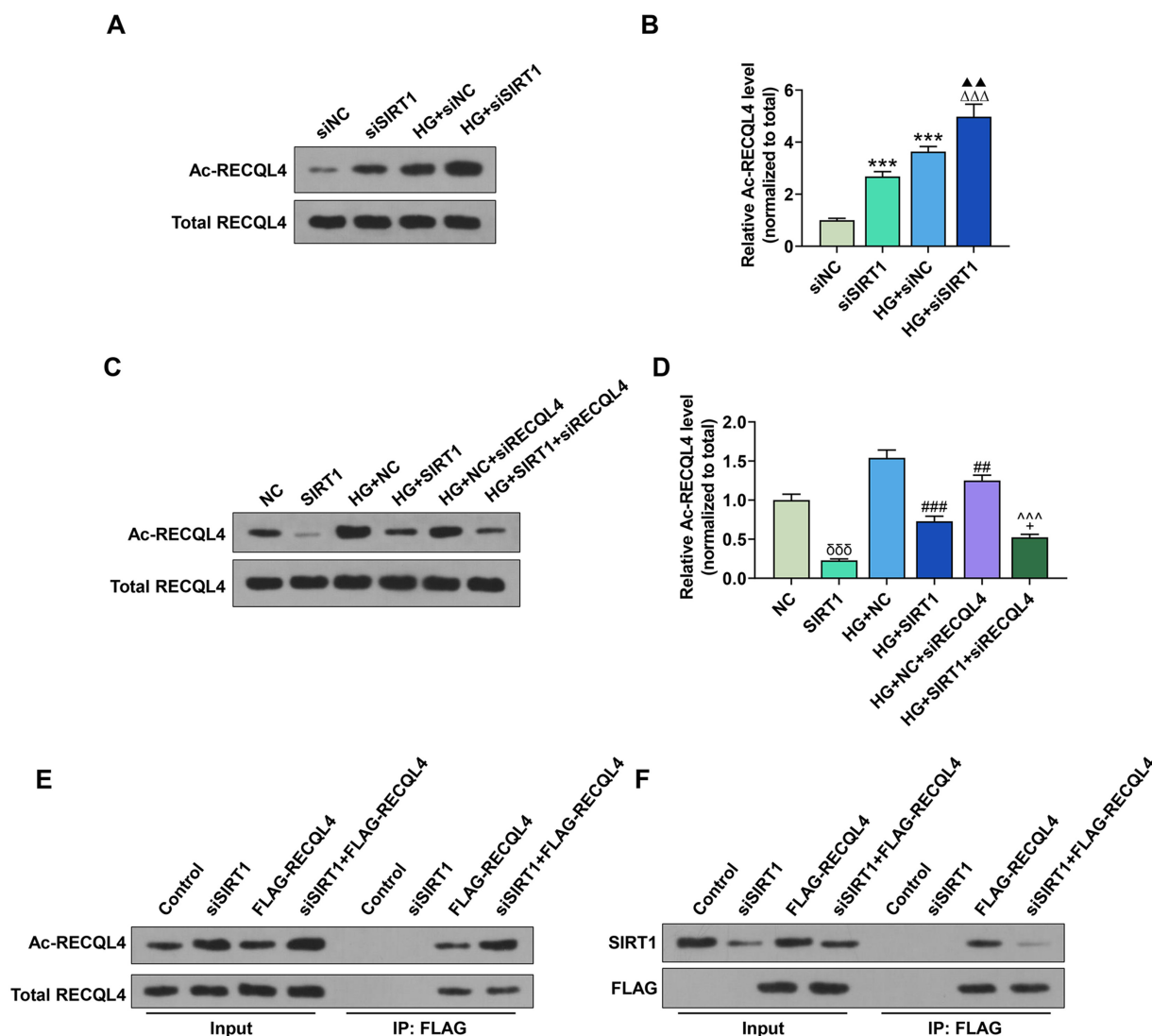


Fig. 6. SIRT1 interacted with and deacetylated RECQL4 in HG-treated osteoblasts. $\delta\delta\delta p < 0.001$, vs. NC; $\#\# p < 0.01$, $\#\#\# p < 0.001$, vs. HG+NC; $\Delta\Delta\Delta p < 0.001$, vs. HG+NC; $\blacktriangle\blacktriangle p < 0.01$, vs. HG+siNC; $+ p < 0.05$, vs. HG+SIRT1; $\wedge\wedge\wedge p < 0.001$, vs. HG+NC+siRECQL4.

the phosphorylation of p53 in osteoblastic cells, suggesting that HG could indeed inhibit the osteogenic differentiation in osteoblastic cells. Hence, it is necessary to further explore this mechanism of HG on the osteogenic differentiation.

By HG stimulation, MMP can be disturbed, ATP production can be reduced, and cell apoptosis can be increased. The results indicate that HG is involved in mitochondrial dysfunction and apoptosis of MC3T3-E1 cells. Additionally, it's worth noting that HG can induce the reduction on the level of GSH, the most abundant thiol referred as the major cellular anti-oxidant and redox regulator, while elevating that of MDA, a known indicator of oxidative stress implicated in lipid peroxidation and is capable to induce MMP depolarization and mitochondrial dysfunction [26–31]. Alters in levels of intracellular anti-oxidative enzymes, including SOD and GSH, may partly account for the HG

induced mitochondrial oxidative stress. RECQL4 is necessary for the transport of p53 into mitochondria in normal human cells without exogenous stress [32]. Furthermore, Kumari *et al.* [13] report that mitochondrial functions of RECQL4 are needed to prevent aerobic glycolysis. Croteau *et al.* [33] state the loss of RECQL4 changes mitochondrial integrity. The findings by Chi *et al.* [34] strongly indicate a regulatory role for RECQL4 in mitochondrial stability and function by evaluating mtDNA copy number and oxidative damage. These findings indicate the role of RECQL4 in mitochondrial function may be involved in DM-related orthopaedic diseases. In this study, we also found that RECQL4 overexpression could reverse the effects of HG on inducing mitochondrial dysfunction, oxidative stress and apoptosis as well as p-p53/p53 of osteoblasts.

The DNA helicase RECQL4 is essential for normal osteoblast expansion and osteosarcoma formation [11]. In our

study, we firstly found that RECQL4 overexpression could reverse the effects of HG on suppressing the osteogenic differentiation of osteoblasts. Improving mitochondrial function promotes osteogenic differentiation of MC3T3-E1 osteoblastic cells [35]. However, these findings are contrary to that of Luo *et al.* [36] who found that mitochondrial dysfunction and autophagy-mediated macrophagic inflammation induced by dicalcium silicate promotes osteogenic differentiation of BMSCs. Therefore, the effects of RECQL4 overexpression on preventing HG suppressing the osteogenic differentiation of osteoblasts may be through attenuating mitochondrial dysfunction.

SIRT1 inhibits HG-induced endothelial injury [37], and SIRT1/Nrf2 signaling activated by fucoxanthin reduces oxidative stress to improve diabetic kidney function and renal fibrosis [38]. Meanwhile, it has been highlighted that HG could increase the histone acetylation yet this trend was blocked by SRT1720 (the potent activator of sirtuin) and that the acetylation of RECQL4 might occur in response to possible oxidative DNA yet SIRT1, a deacetylase promoting the osteogenic differentiation in mice, could deacetylate RECQL4 in osteosarcoma cell line U2OS [16–19]. Consistent with the literature [19], this research found that SIRT1 interacts with and deacetylates RECQL4. HG significantly inhibited the osteogenic differentiation of osteoblasts via regulating SIRT1/RECQL4 axis. Similarly, SIRT6 significantly suppresses HG-induced mitochondrial dysfunction and apoptosis in podocytes [39].

Taken together, the present study indicated that the regulatory effect of SIRT1/RECQL4 axis on HG-caused osteogenic differentiation of osteoblasts could be attributed to the inhibition of mitochondrial dysfunction, including reducing oxidative stress and apoptosis and increasing MMP. However, we did not explore downstream molecules of SIRT1/RECQL4 axis that may also contribute to the modulation of mitochondrial function and apoptosis during osteogenic differentiation of osteoblasts. The roles of HG and its interaction with SIRT1/RECQL4 axis in osteoblasts were only confirmed based on the cellular model *in vitro*. The goal to validate these results using animal model *in vivo*. Our results indicated that SIRT1/RECQL4 axis might be regarded as a potential therapeutic target for the treatment of DM-associated bone disease in clinical settings. It's hoped that this study can contribute to bringing further insights into the role of HG on osteoblasts and figuring out potential preventive and therapeutic methods for DM-associated bone disease in the future.

Conclusions

The aim of this study was explore the mechanism of the effects of HG on the osteogenic differentiation of osteoblasts. The study showed that HG could suppress the osteogenic differentiation and induce mitochondrial dysfunction of osteoblasts, which was achieved by regulating SIRT1/RECQL4 axis.

Availability of Data and Materials

The analyzed data sets generated during the study are available from the corresponding author on reasonable request.

Author Contributions

XZ and WP—has made the design of the work and written this article; XZ, WP, SP, ZL, RP and QW—have done the acquisition, analysis, and interpretation of data. All authors have drafted the work and substantively revised it. All authors read and approved the final manuscript.

Ethics Approval and Consent to Participate

Not applicable.

Acknowledgment

Not applicable.

Funding

This work was supported by the Research on TCM Health Rehabilitation Intervention Strategy for Patients with Osteoporosis in Wenzhou Community [2018ZY017].

Conflict of Interest

The authors declare no conflict of interest.

References

- [1] Wang A, Green JB, Halperin JL, Piccini JP. Atrial Fibrillation and Diabetes Mellitus. *Journal of the American College of Cardiology*. 2019; 74: 1107–1115.
- [2] Hozayen WG, Mahmoud AM, Soliman HA, Mostafa SR. Spirulina versicolor improves insulin sensitivity and attenuates hyperglycemia-mediated oxidative stress in fructose-fed rats. *Journal of Intercultural Ethnopharmacology*. 2016; 5: 57–64.
- [3] Paschou SA, Vryonidou A. Diabetes mellitus and osteoporosis. *Minerva Endocrinologica*. 2020; 44: 333–335.
- [4] Rehling T, Björkman AD, Andersen MB, Ekholm O, Molsted S. Diabetes is Associated with Musculoskeletal Pain, Osteoarthritis, Osteoporosis, and Rheumatoid Arthritis. *Journal of Diabetes Research*. 2019; 2019: 6324348.
- [5] Kim JM, Lin C, Stavre Z, Greenblatt MB, Shim JH. Osteoblast-Osteoclast Communication and Bone Homeostasis. *Cells*. 2020; 9: 2073.
- [6] Lee W, Guntur AR, Long F, Rosen CJ. Energy Metabolism of the Osteoblast: Implications for Osteoporosis. *Endocrine Reviews*. 2017; 38: 255–266.
- [7] Yang J, Ma C, Zhang M. High glucose inhibits osteogenic differentiation and proliferation of MC3T3-E1 cells by regulating P2X7. *Molecular Medicine Reports*. 2019; 20: 5084–5090.
- [8] Dong K, Hao P, Xu S, Liu S, Zhou W, Yue X, *et al.* Alpha-Lipoic Acid Alleviates High-Glucose Suppressed Osteogenic Differentiation of MC3T3-E1 Cells via Antioxidant Effect and PI3K/Akt Signaling Pathway. *Cellular Physiology and Biochemistry*. 2017; 42: 1897–1906.

- [9] Sun M, Yang J, Wang J, Hao T, Jiang D, Bao G, *et al.* TNF- α is upregulated in T2DM patients with fracture and promotes the apoptosis of osteoblast cells *in vitro* in the presence of high glucose. *Cytokine*. 2016; 80: 35–42.
- [10] Bailey MH, Tokheim C, Porta-Pardo E, Sengupta S, Bertrand D, Weerasinghe A, *et al.* Comprehensive Characterization of Cancer Driver Genes and Mutations. *Cell*. 2018; 174: 1034–1035.
- [11] Ng AJ, Walia MK, Smeets MF, Mutsaers AJ, Sims NA, Purton LE, *et al.* The DNA helicase recq4 is required for normal osteoblast expansion and osteosarcoma formation. *PLoS Genetics*. 2015; 11: e1005160.
- [12] Lu L, Harutyunyan K, Jin W, Wu J, Yang T, Chen Y, *et al.* RECQL4 Regulates p53 Function *in Vivo* during Skeletogenesis. *Journal of Bone and Mineral Research*. 2015; 30: 1077–1089.
- [13] Kumari J, Hussain M, De S, Chandra S, Modi P, Tikoo S, *et al.* Mitochondrial functions of RECQL4 are required for the prevention of aerobic glycolysis-dependent cell invasion. *Journal of Cell Science*. 2016; 129: 1312–1318.
- [14] Baeza J, Smallegan MJ, Denu JM. Mechanisms and Dynamics of Protein Acetylation in Mitochondria. *Trends in Biochemical Sciences*. 2016; 41: 231–244.
- [15] Narita T, Weinert BT, Choudhary C. Functions and mechanisms of non-histone protein acetylation. *Nature Reviews Molecular Cell Biology*. 2019; 20: 156–174.
- [16] Yu J, Wu Y, Yang P. High glucose-induced oxidative stress represses sirtuin deacetylase expression and increases histone acetylation leading to neural tube defects. *Journal of Neurochemistry*. 2016; 137: 371–383.
- [17] Su C, Wang Q, Luo H, Jiao W, Tang J, Li L, *et al.* Si-Miao-Yong-An decoction attenuates cardiac fibrosis via suppressing TGF- β 1 pathway and interfering with MMP-TIMPs expression. *Biomedicine & Pharmacotherapy = Biomédecine & Pharmacothérapie*. 2020; 127: 110132.
- [18] Wang H, Hu Z, Wu J, Mei Y, Zhang Q, Zhang H, *et al.* Sirt1 Promotes Osteogenic Differentiation and Increases Alveolar Bone Mass via Bmi1 Activation in Mice. *Journal of Bone and Mineral Research*. 2019; 34: 1169–1181.
- [19] Duan S, Han X, Akbari M, Croteau DL, Rasmussen L, Bohr VA. Interaction between RECQL4 and OGG1 promotes repair of oxidative base lesion 8-oxoG and is regulated by SIRT1 deacetylase. *Nucleic Acids Research*. 2020; 48: 6530–6546.
- [20] Wang T, Kang W, Du L, Ge S. Rho-kinase inhibitor Y-27632 facilitates the proliferation, migration and pluripotency of human periodontal ligament stem cells. *Journal of Cellular and Molecular Medicine*. 2017; 21: 3100–3112.
- [21] Huang H, Shi Y, He H, Wang Y, Chen T, Yang L, *et al.* MiR-4673 Modulates Paclitaxel-Induced Oxidative Stress and Loss of Mitochondrial Membrane Potential by Targeting 8-Oxoguanine-DNA Glycosylase-1. *Cellular Physiology and Biochemistry*. 2017; 42: 889–900.
- [22] Ma J, Kang SY, Meng X, Kang AN, Park JH, Park YK, *et al.* Effects of Rhizome Extract of *Dioscorea batatas* and its Active Compound, Allantoin, on the Regulation of Myoblast Differentiation and Mitochondrial Biogenesis in C2C12 Myotubes. *Molecules (Basel, Switzerland)*. 2018; 23: 2023.
- [23] Wang Y, Sun H, Song J, Yao G, Sun H, Ge Z. MiR-139-5p protect against myocardial ischemia and reperfusion (I/R) injury by targeting autophagy-related 4D and inhibiting AMPK/mTOR/ULK1 pathway. *International Journal of Clinical and Experimental Pathology*. 2017; 10: 10140–10151.
- [24] Sarbishegi M, Alhagh Charkhat Gorgich E, Khajavi O. Olive Leaves Extract Improved Sperm Quality and Antioxidant Status in the Testis of Rat Exposed to Rotenone. *Nephro-Urology Monthly*. 2017; 9: e47127.
- [25] Livak KJ, Schmittgen TD. Analysis of relative gene expression data using real-time quantitative PCR and the 2(-Delta Delta C(T)) Method. *Methods (San Diego, Calif.)*. 2001; 25: 402–408.
- [26] Ferguson GD, Bridge WJ. The glutathione system and the related thiol network in *Caenorhabditis elegans*. *Redox Biology*. 2019; 24: 101171.
- [27] Garcia J, Han D, Sancheti H, Yap L, Kaplowitz N, Cadenas E. Regulation of Mitochondrial Glutathione Redox Status and Protein Glutathionylation by Respiratory Substrates. *Journal of Biological Chemistry*. 2010; 285: 39646–39654.
- [28] Liu X, Han S, Yang Y, Kang J, Wu J. Glucose-induced glutathione reduction in mitochondria is involved in the first phase of pancreatic β -cell insulin secretion. *Biochemical and Biophysical Research Communications*. 2015; 464: 730–736.
- [29] Caruso G, Benatti C, Blom JMC, Caraci F, Tasciedda F. The Many Faces of Mitochondrial Dysfunction in Depression: From Pathology to Treatment. *Frontiers in Pharmacology*. 2019; 10: 995.
- [30] Cheng J, Wang F, Yu D, Wu P, Chen J. The cytotoxic mechanism of malondialdehyde and protective effect of carnosine via protein cross-linking/mitochondrial dysfunction/reactive oxygen species/MAPK pathway in neurons. *European Journal of Pharmacology*. 2011; 650: 184–194.
- [31] Chen Q, Tang L, Xin G, Li S, Ma L, Xu Y, *et al.* Oxidative stress mediated by lipid metabolism contributes to high glucose-induced senescence in retinal pigment epithelium. *Free Radical Biology and Medicine*. 2019; 130: 48–58.
- [32] De S, Kumari J, Mudgal R, Modi P, Gupta S, Futami K, *et al.* RECQL4 is essential for the transport of p53 to mitochondria in normal human cells in the absence of exogenous stress. *Journal of Cell Science*. 2012; 125: 2509–2522.
- [33] Croteau DL, Rossi ML, Canugovi C, Tian J, Sykora P, Rammamorthy M, *et al.* RECQL4 localizes to mitochondria and preserves mitochondrial DNA integrity. *Aging Cell*. 2012; 11: 456–466.
- [34] Chi Z, Nie L, Peng Z, Yang Q, Yang K, Tao J, *et al.* RecQL4 cytoplasmic localization: Implications in mitochondrial DNA oxidative damage repair. *The International Journal of Biochemistry & Cell Biology*. 2012; 44: 1942–1951.
- [35] Zhai Y, Behera J, Tyagi SC, Tyagi N. Hydrogen sulfide attenuates homocysteine-induced osteoblast dysfunction by inhibiting mitochondrial toxicity. *Journal of Cellular Physiology*. 2019; 234: 18602–18614.
- [36] Luo Q, Li X, Zhong W, Cao W, Zhu M, Wu A, *et al.* Dicalcium silicate-induced mitochondrial dysfunction and autophagy-mediated macrophagic inflammation promotes osteogenic differentiation of BMSCs. *Regenerative Biomaterials*. 2021; 9: rbab075.
- [37] Qin R, Zhang L, Lin D, Xiao F, Guo L. Sirt1 inhibits HG-induced endothelial injury: Role of Mff-based mitochondrial fission and F-actin homeostasis-mediated cellular migration. *International Journal of Molecular Medicine*. 2019; 44: 89–102.
- [38] Yang G, Li Q, Peng J, Jin L, Zhu X, Zheng D, *et al.* Fucoxanthin regulates Nrf2 signaling to decrease oxidative stress and improves renal fibrosis depending on Sirt1 in HG-induced GMCs and STZ-induced diabetic rats. *European Journal of Pharmacology*. 2021; 913: 174629.
- [39] Fan Y, Yang Q, Yang Y, Gao Z, Ma Y, Zhang L, *et al.* Sirt6 Suppresses High Glucose-Induced Mitochondrial Dysfunction and Apoptosis in Podocytes through AMPK Activation. *International Journal of Biological Sciences*. 2019; 15: 701–713.